PHYSICAL REVIEW D **96,** 063517 (2017)

Conjoined constraints on modified gravity from the expansion history and cosmic growth

Spyros Basilakos[1,*] and Savvas Nesseris[2,†]

[1]*Academy of Athens, Research Center for Astronomy and Applied Mathematics, Soranou Efesiou 4, 11527 Athens, Greece*

[2]*Instituto de Física Teórica UAM-CSIC, Universidad Autonóma de Madrid, Cantoblanco, 28049 Madrid, Spain*

(Received 24 May 2017; published 18 September 2017)

In this paper we present conjoined constraints on several cosmological models from the expansion history $H(z)$ and cosmic growth $f\sigma_8$. The models we study include the CPL w_0w_a parametrization, the holographic dark energy (HDE) model, the time-varying vacuum (Λ_tCDM) model, the Dvali, Gabadadze and Porrati (DGP) and Finsler-Randers (FRDE) models, a power-law $f(T)$ model, and finally the Hu-Sawicki $f(R)$ model. In all cases we perform a simultaneous fit to the SnIa, CMB, BAO, $H(z)$ and growth data, while also following the conjoined visualization of $H(z)$ and $f\sigma_8$ as in Linder (2017). Furthermore, we introduce the figure of merit (FoM) in the $H(z)$-$f\sigma_8$ parameter space as a way to constrain models that jointly fit both probes well. We use both the latest $H(z)$ and $f\sigma_8$ data, but also LSST-like mocks with 1% measurements, and we find that the conjoined method of constraining the expansion history and cosmic growth simultaneously is able not only to place stringent constraints on these parameters, but also to provide an easy visual way to discriminate cosmological models. Finally, we confirm the existence of a tension between the growth-rate and Planck CMB data, and we find that the FoM in the conjoined parameter space of $H(z)$-$f\sigma_8(z)$ can be used to discriminate between the ΛCDM model and certain classes of modified gravity models, namely the DGP and $f(T)$.

DOI: 10.1103/PhysRevD.96.063517

I. INTRODUCTION

The portrait of the cosmos, as it is revealed by the analysis of various independent cosmological observations (see Ref. [1] and references therein), is tightly tied with a spatially flat Universe in which the cosmic fluid contains ∼30% of matter (baryonic and dark) and the rest is the so-called dark energy (DE). Although there is mounting observational evidence that DE is responsible for the accelerated expansion of the Universe, the underlying mechanism behind such a phenomenon is yet unknown.

Despite the lack of our knowledge regarding the nature of the DE, in the literature there is a large class of cosmological models which mathematically treats the accelerated expansion of the Universe. In general, these cosmological scenarios are split into two large groups. The first category of DE models adhere to general relativity (GR) and propose the existence of new fields in nature (for review, see Refs. [2,3] and references therein). The second group of cosmological models is mainly based on modified gravity for which the present accelerating era appears as a geometric effect due to the fact that gravity becomes weak at cosmological scales [2,4]. It is interesting to mention that in the context of modified gravity models, the effective equation of state (EoS) parameter can enter in the phantom regime, namely $w < -1$.

At the perturbation level, the growth of matter fluctuation provides a useful tool to investigate the matter distribution in the Universe [5], and, more importantly, it can be measured from observations. Indeed, the growth-rate data are mainly based on galaxy surveys, like SDSS, BOSS, WiggleZ, etc. (see our Table II and references therein). The growth-rate data have been used extensively in the literature in order to put constraints on the growth index γ. The measurement of the growth index provides an efficient way to discriminate between modified gravity models and DE models which are developed in the context of GR. Indeed, one can find a large family of studies in which the predicted growth index is given analytically for various DE models, including scalar-field DE [6–10], DGP [9,11,12], $f(R)$ [13–15], Finsler-Randers [16], time-varying vacuum models $\Lambda(H)$ [17], clustered DE [18], holographic dark energy [19] and $f(T)$ [20].

From the aforementioned discussion, it becomes clear that up to now, the expansion data and the growth data have been used separately in order to study the cosmic history at the background and perturbations levels, respectively. In this article we follow a different path, namely the *conjoined method* recently proposed by Linder [21], where it was claimed that in order to distinguish the DE models, it is better to use the Hubble parameter $H(z)$ directly with the growth quantity $f\sigma_8(z)$ in a conjoined diagram, rather than

*svasil@academyofathens.gr
†savvas.nesseris@csic.es

using each as a function of redshift. In the current article we attempt to investigate such a possibility by computing the H-$f\sigma_8$ diagram of the most popular DE models and comparing the corresponding predictions with the observed conjoined diagram provided by the cosmic chronometer $H(z)$ and the growth data. A similar, but not overlapping, analysis of the conjoined constraints was also made by Ref. [22], where the authors studied extensions of the ΛCDM model, such as a constant but free equation of state w or the effect of neutrinos. However, we consider a much bigger ensemble of dark energy models, hence our analysis is much more broad in scope.

The layout of the article is as follows: In Sec. II we discuss the linear growth of matter fluctuations in the dark energy regime, while in Sec. III we present the basic properties of various cosmological models, including those of modified gravity. In Sec. IV we discuss the tension between the growth and Planck15 CMB data, while in Sec. V, we test the DE cosmologies by comparing the theoretical predictions of the conjoined H-$f\sigma_8$ diagram with observations. Finally, we present our conclusions in Sec. VI.

II. LINEAR GROWTH OF MATTER PERTURBATIONS

In this section we present the main ingredients of the linear growth of matter perturbations within the context of different types of dark energy. Since we are in the matter-dominated epoch, we can neglect the radiation component from the cosmic expansion. Let us start the current analysis with the basic differential equation at subhorizon scales [9,11,13,23–25]:

$$\ddot{\delta}_m + 2\tilde{\nu}H\dot{\delta}_m - 4\pi G\mu\rho_m\delta_m = 0. \tag{1}$$

As is well known, a general solution of the aforementioned equation is written as $\delta_m \propto D(t)$. Notice that $D(t)$ is the growth factor, usually scaled to unity at the present time. In order to address the issue of how the quantities $\tilde{\nu}$ and $\mu \equiv G_{\rm eff}/G_N$ affect the matter fluctuations, one has to deal in general with the following three distinct scenarios:

(1) The situation in which the dark energy models (quintessence and the like) adhere to GR, hence $(\tilde{\nu}, \mu) = (1, 1)$.
(2) The case where $(\tilde{\nu}, \mu) \neq (1, 1)$, which implies that there are interactions in the dark sector.
(3) The case of either modified gravity models or inhomogeneous dark energy models (inside GR), hence $\tilde{\nu} = 1$ and $\mu \neq 1$.[1]

Now we are ready to introduce the growth rate of clustering (first proposed by Ref. [27]) as follows:

$$f(a) = \frac{d\ln\delta_m}{d\ln a} \simeq \Omega_m^{\gamma}(a), \tag{2}$$

with

$$\Omega_m(a) = \frac{\Omega_{m0}a^{-3}}{E^2(a)}, \tag{3}$$

where $E(a) = H(a)/H_0$ is the normalized Hubble parameter and γ is the growth index. By differentiating Eq. (3), it is easy to show

$$\frac{d\Omega_m}{da} = -3\frac{\Omega_m(a)}{a}\left(1 + \frac{2}{3}\frac{d\ln E}{d\ln a}\right). \tag{4}$$

Furthermore, combining Eqs. (2)–(4), the main equation (1) becomes

$$a\frac{df}{da} + \left(2\tilde{\nu} + \frac{d\ln E}{d\ln a}\right)f + f^2 = \frac{3\mu\Omega_m}{2}, \tag{5}$$

or

$$a\ln(\Omega_m)\frac{d\gamma}{da} + \Omega_m^{\gamma} - 3\gamma + 2\tilde{\nu} - \left(\gamma - \frac{1}{2}\right)\frac{d\ln E}{d\ln a} = \frac{3}{2}\mu\Omega_m^{1-\gamma}. \tag{6}$$

It is interesting to mention that Steigerwald *et al.* [28] have provided another expression of the above equation, namely

$$\frac{d\omega}{d\ln a}\left(\gamma + \omega\frac{d\gamma}{d\omega}\right) + e^{\omega\gamma} + 2\tilde{\nu} + \frac{d\ln E}{d\ln a} = \frac{3}{2}\mu e^{\omega(1-\gamma)}, \tag{7}$$

where $\omega = \ln\Omega_m(a)$, which implies that at $z \gg 1$ $(a \to 0)$ we get $\Omega_m(a) \to 1$ (or $\omega \to 0$). Based on Eq. (7), Steigerwald *et al.* [28] proposed a general mathematical approach in order to derive the asymptotic value of the growth index, which is given by [see Eq. (8) in Ref. [28] and the relevant discussion in Ref. [17]]

$$\gamma_\infty = \frac{3(M_0 + M_1) - 2(H_1 + N_1)}{2 + 2X_1 + 3M_0}, \tag{8}$$

where

$$M_0 = \mu|_{\omega=0}, \qquad M_1 = \left.\frac{d\mu}{d\omega}\right|_{\omega=0}, \tag{9}$$

and

$$N_1 = \left.\frac{d\tilde{\nu}}{d\omega}\right|_{\omega=0} \qquad H_1 = -\frac{X_1}{2} = \left.\frac{d(d\ln E/d\ln a)}{d\omega}\right|_{\omega=0}. \tag{10}$$

Since the exact functional form of the growth index has yet to be found, here we utilize the well-known Taylor expansion around $a(z) = 1$ (see Refs. [29–31]):

[1]Note that if matter and geometry are coupled, then we have $\mu \equiv G_{\rm eff}/G_N + \beta(a, k)$, in which $\beta(a, k)$ is a quantity that depends on derivatives of the Lagrangian of the model [26].

$$\gamma(a) = \gamma_0 + \gamma_1(1-a), \tag{11}$$

in which the asymptotic value boils down to $\gamma_\infty \simeq \gamma_0 + \gamma_1$, where we have set $\gamma_0 = \gamma(1)$. Lastly, writing Eq. (6) at the present time ($a = 1$),

$$-\gamma'(1)\ln(\Omega_{m0}) + \Omega_{m0}^{\gamma(1)} - 3\gamma(1) + 2\tilde{\nu}_0 - 2\left(\gamma_0 - \frac{1}{2}\right)\frac{d\ln E}{d\ln a}\bigg|_{a=1} = \frac{3}{2}\mu_0\Omega_{m0}^{1-\gamma(1)}, \tag{12}$$

and with the aid of Eq. (11), we arrive at

$$\gamma_1 = \frac{\Omega_{m0}^{\gamma_0} - 3\gamma_0 + 2\tilde{\nu}_0 - 2(\gamma_0 - \frac{1}{2})\frac{d\ln E}{d\ln a}|_{a=1} - \frac{3}{2}\mu_0\Omega_{m0}^{1-\gamma_0}}{\ln\Omega_{m0}}, \tag{13}$$

where a prime denotes a derivative with respect to the scale factor, $\mu_0 = \mu(1)$, and $\tilde{\nu}_0 = \tilde{\nu}(1)$.

III. DARK ENERGY MODELS

In this section, we describe the ten distinct cosmological models used in our analysis. Notice that the observational viability of these DE models was recently tested in Basilakos and Nesseris [32] using the JLA supernovae, the BAO data, and the CMB shift parameters, but also the $H(z)$ data shown in Table I. We also used a growth-rate data compilation which we now update to the "Gold-2017" set of Ref. [33], shown for completeness in Table II. For the details of the analysis of the JLA, BAO, CMB and $H(z)$ data, we refer the interested reader to Ref. [32], while for that of the new growth-rate data, we refer to Ref. [33]. The best-fit parameters and their errors for all of the models used in this analysis were obtained via an MCMC, and the results are shown in Table III.[2]

Knowing the basic cosmological functions of a given dark energy model and the corresponding model parameters, it is trivial to compute the asymptotic value of the growth index γ_∞ from Eq. (8). The next step is to solve the system of $\gamma_\infty = \gamma_0 + \gamma_1$ and Eq. (13) in order to compute (γ_0, γ_1) from the cosmological parameters. Let us now briefly present the cosmological models explored in the current work. Notice that in all cases we assume a spatially flat Friedmann-Lemaître-Robertson-Walker (FLRW) geometry.

(1) ***w*CDM model:** In this case, we consider as constant the equation-of-state (hereafter EoS) parameter $w = p_d/\rho_d$, where p_d and ρ_d are the pressure and density of the dark energy fluid, respectively. Since this model is inside GR and does not allow interactions in the dark sector, we have $\mu(a) = \tilde{\nu}(a) = 1$.

[2]The codes used in the analysis are freely available at www.uam.es/savvas.nesseris/.

TABLE I. The $H(z)$ data used in the current analysis (in units of $\mathrm{km\,s^{-1}\,Mpc^{-1}}$). This compilation is based partly on those of Refs. [34,35].

z	$H(z)$	σ_H	References
0.07	69.0	19.6	[36]
0.09	69.0	12.0	[37]
0.12	68.6	26.2	[36]
0.17	83.0	8.0	[37]
0.179	75.0	4.0	[38]
0.199	75.0	5.0	[38]
0.2	72.9	29.6	[36]
0.27	77.0	14.0	[37]
0.28	88.8	36.6	[36]
0.35	82.7	8.4	[39]
0.352	83.0	14.0	[38]
0.3802	83.0	13.5	[34]
0.4	95.0	17.0	[37]
0.4004	77.0	10.2	[34]
0.4247	87.1	11.2	[34]
0.44	82.6	7.8	[40]
0.44497	92.8	12.9	[34]
0.4783	80.9	9.0	[34]
0.48	97.0	62.0	[37]
0.57	96.8	3.4	[41]
0.593	104.0	13.0	[38]
0.60	87.9	6.1	[40]
0.68	92.0	8.0	[38]
0.73	97.3	7.0	[40]
0.781	105.0	12.0	[38]
0.875	125.0	17.0	[38]
0.88	90.0	40.0	[37]
0.9	117.0	23.0	[37]
1.037	154.0	20.0	[38]
1.3	168.0	17.0	[37]
1.363	160.0	33.6	[42]
1.43	177.0	18.0	[37]
1.53	140.0	14.0	[37]
1.75	202.0	40.0	[37]
1.965	186.5	50.4	[42]
2.34	222.0	7.0	[43]

The latter conditions imply that the dimensionless Hubble parameter is written as

$$E^2(a) = \Omega_{m0}a^{-3} + \Omega_{d0}a^{-3(1+w)}, \tag{14}$$

where the model parameters are $\Omega_{m0} = 1 - \Omega_{d0}$ and w. Using Eq. (14), we find

$$\frac{d\ln E}{d\ln a} = -\frac{3}{2} - \frac{3}{2}w[1 - \Omega_m(a)] \tag{15}$$

and

$$\{M_0, M_1, H_1, X_1\} = \left\{1, 0, \frac{3w}{2}, -3w\right\}.$$

TABLE II. A compilation of robust and independent $f\sigma_8(z)$ measurements from different surveys, compiled in Ref. [33]. In the columns, we show in ascending order, with respect to redshift, the name and year of the survey that made the measurement, the redshift and value of $f\sigma_8(z)$, and the corresponding reference and fiducial cosmology. These data points are used in our analysis in the next sections.

Index	Data set	z	$f\sigma_8(z)$	References	Year	Notes
1	6dFGS + SnIa	0.02	0.428 ± 0.0465	[44]	2016	$(\Omega_m, h, \sigma_8) = (0.3, 0.683, 0.8)$
2	SnIa + IRAS	0.02	0.398 ± 0.065	[45,46]	2011	$(\Omega_m, \Omega_K) = (0.3, 0)$
3	2MASS	0.02	0.314 ± 0.048	[46,47]	2010	$(\Omega_m, \Omega_K) = (0.266, 0)$
4	SDSS-veloc	0.10	0.370 ± 0.130	[48]	2015	$(\Omega_m, \Omega_K) = (0.3, 0)$
5	SDSS-MGS	0.15	0.490 ± 0.145	[49]	2014	$(\Omega_m, h, \sigma_8) = (0.31, 0.67, 0.83)$
6	2dFGRS	0.17	0.510 ± 0.060	[50]	2009	$(\Omega_m, \Omega_K) = (0.3, 0)$
7	GAMA	0.18	0.360 ± 0.090	[51]	2013	$(\Omega_m, \Omega_K) = (0.27, 0)$
8	GAMA	0.38	0.440 ± 0.060	[51]	2013	
9	SDSS-LRG-200	0.25	0.3512 ± 0.0583	[52]	2011	$(\Omega_m, \Omega_K) = (0.25, 0)$
10	SDSS-LRG-200	0.37	0.4602 ± 0.0378	[52]	2011	
11	BOSS-LOWZ	0.32	0.384 ± 0.095	[53]	2013	$(\Omega_m, \Omega_K) = (0.274, 0)$
12	SDSS-CMASS	0.59	0.488 ± 0.060	[54]	2013	$(\Omega_m, h, \sigma_8) = (0.307115, 0.6777, 0.8288)$
13	WiggleZ	0.44	0.413 ± 0.080	[40]	2012	$(\Omega_m, h) = (0.27, 0.71)$
14	WiggleZ	0.60	0.390 ± 0.063	[40]	2012	
15	WiggleZ	0.73	0.437 ± 0.072	[40]	2012	
16	Vipers PDR-2	0.60	0.550 ± 0.120	[55]	2016	$(\Omega_m, \Omega_b) = (0.3, 0.045)$
17	Vipers PDR-2	0.86	0.400 ± 0.110	[55]	2016	
18	FastSound	1.40	0.482 ± 0.116	[5]	2015	$(\Omega_m, \Omega_K) = (0.270, 0)$

Inserting the above coefficients into Eq. (8), we recover the well-known asymptotic value of the growth index (see also Refs. [6–11,56]), namely

$$\gamma_\infty = \frac{3(w-1)}{6w-5}.$$

As expected for $w = -1$, the wCDM model reduces to a ΛCDM cosmological model in which $\gamma_\infty^{(\Lambda)} = 6/11$.

(2) **CPL model (w_0w_aCDM):** This phenomenological model was first proposed by Chevalier, Polarski, and Linder [57,58]. Specifically, the dark energy EoS parameter is given as a first-order Taylor expansion around the present epoch, $w(a) = w_0 + w_1(1-a)$. This model shares the same cosmological properties with wCDM, which means that $\mu(a) = \tilde{\nu}(a) = 1$. The normalized Hubble parameter is given by

$$E^2(a) = \Omega_{m0}a^{-3} + \Omega_{d0}a^{-3(1+w_0+w_1)}e^{3w_1(a-1)},$$

where the free parameters of the models are (Ω_{m0}, w_0, w_1), with $\Omega_{d0} = 1 - \Omega_{m0}$. The quantity $d\ln E/d\ln a$ is given by Eq. (15), but here the EoS parameter is $w = w(a)$. Within this context, the growth coefficients (see also Ref. [28]) are written as

$$\{M_0, M_1, H_1, X_1\} = \left\{1, 0, \frac{3(w_0+w_1)}{2}, -3(w_0+w_1)\right\},$$

and thus

$$\gamma_\infty = \frac{3(w_0+w_1-1)}{6(w_0+w_1)-5}.$$

(3) **Running Λ (Λ_tCDM model):** Here we allow Λ to vary with redshift. Using the notations of Refs. [59,60], the evolution of the vacuum is written as $\Lambda(H) = \Lambda_0 + 3\nu(H^2 - H_0^2)$, where $\Lambda_0 \equiv \Lambda(H_0) = 3\Omega_{\Lambda 0}H_0^2$. In this case the normalized Hubble parameter takes the form

$$E^2(a) = \tilde{\Omega}_{\Lambda 0} + \tilde{\Omega}_{m0}a^{-3(1-\nu)}, \tag{16}$$

with

$$\frac{d\ln E}{d\ln a} = -\frac{3}{2}(1-\nu)\tilde{\Omega}_m(a), \tag{17}$$

where we have set $\tilde{\Omega}_m(a) = \frac{\tilde{\Omega}_{m0}a^{-3(1-\nu)}}{E^2(a)}$, $\tilde{\Omega}_{m0} \equiv \frac{\Omega_{m0}}{1-\nu}$ and $\tilde{\Omega}_{\Lambda 0} \equiv \frac{1-\Omega_{m0}-\nu}{1-\nu}$. Evidently, the free parameters of the model are $(\tilde{\Omega}_{m0}, \nu)$. The basic quantities $\tilde{\nu}$ and μ (see Ref. [17]) are given by

$$\tilde{\nu} = 1 + \frac{3}{2}\nu \tag{18}$$

and

$$\mu(a) = 1 - \nu - \frac{4\nu}{\tilde{\Omega}_m(a)} + 3\nu(1-\nu). \tag{19}$$

TABLE III. The best-fit parameters of the various parameters of the models presented in the previous section.

Model	α	β	Ω_m	$\Omega_b h^2$	γ_0	γ_1	DE params.	h	σ_8	$\chi^2_{\rm min}$
ΛCDM	0.141 ± 0.006	3.102 ± 0.004	0.315 ± 0.003	0.0222 ± 0.0001	0.725 ± 0.036	0.584 ± 0.127	$w_0 = -1$ $w_a = 0$	0.673 ± 0.002	0.877 ± 0.034	743.303
wCDM	0.141 ± 0.005	3.097 ± 0.005	0.318 ± 0.004	0.0223 ± 0.0004	0.731 ± 0.069	0.581 ± 0.058	$w_0 = -0.987 \pm 0.005$ $w_a = 0$	0.670 ± 0.003	0.879 ± 0.033	743.235
CPL	0.141 ± 0.004	3.100 ± 0.005	0.317 ± 0.006	0.0222 ± 0.0001	0.729 ± 0.036	0.576 ± 0.118	$w_0 = -0.984 \pm 0.008$ $w_a = -0.020 \pm 0.004$	0.671 ± 0.004	0.878 ± 0.036	743.248
DGP	0.136 ± 0.006	3.076 ± 0.017	0.390 ± 0.006	0.0229 ± 0.0001	1.053 ± 0.074	0.900 ± 0.092	…	0.588 ± 0.003	1.028 ± 0.046	844.348
Time Var.	0.141 ± 0.008	3.076 ± 0.008	0.319 ± 0.004	0.0222 ± 0.0001	0.737 ± 0.064	0.669 ± 0.123	$s = (-2.95 \pm 13.6) \times 10^{-5}$	0.671 ± 0.004	0.886 ± 0.058	743.689
Holo.	0.142 ± 0.005	3.092 ± 0.008	0.314 ± 0.003	0.0224 ± 0.0001	0.740 ± 0.055	0.832 ± 0.055	$v = 0.669 \pm 0.008$	0.669 ± 0.002	0.896 ± 0.047	751.237
$f(R)$	0.141 ± 0.005	3.110 ± 0.013	0.317 ± 0.005	0.0222 ± 0.0001	0.753 ± 0.041	0.690 ± 0.062	$b = 0.083 \pm 0.005$	0.671 ± 0.003	0.896 ± 0.032	743.337
$f(T)$	0.141 ± 0.008	3.095 ± 0.027	0.317 ± 0.005	0.0222 ± 0.0001	0.730 ± 0.091	0.586 ± 0.067	$b = 0.021 \pm 0.013$	0.671 ± 0.003	0.879 ± 0.057	743.230

Based on the above, we compute the growth coefficients [17]

$$\{M_0, M_1, H_1, X_1\} = \left\{1 - 2\nu - 3\nu^2, -\frac{3(1-\nu)}{2}, 3(1-\nu)\right\},$$

from which we provide

$$\gamma_\infty = \frac{6 + 3\nu}{11 - 12\nu}.$$

(4) **Holographic dark energy (HDE) model:** Using the holographic [61,62] principle in GR $\tilde{\nu}(a) = 1$, one can show that

$$w(a) = -\frac{1}{3} - \frac{2\sqrt{\Omega_{\rm d}(a)}}{3s}$$

and

$$\frac{d\ln\Omega_d}{d\ln a} = -\frac{w(a)}{3}[1 - \Omega_d(a)]$$

and

$$E^2(a) = \frac{\Omega_{m0}a^{-3}}{1 - \Omega_d(a)},$$

where $\Omega_d(a) = 1 - \Omega_m(a)$. Here the cosmological parameters are Ω_{m0} and s. Note that the expression of $d\ln E/d\ln a$ is given by Eq. (14). We would like to stress that the aforementioned three equations produce a system whose solution provides $w(a)$, $\Omega_d(a)$ and $E(a)$.

The intrinsic features of the HDE are characterized by the quantity $\mu(a)$ as follows [19]:

$$\mu(a) = \begin{cases} 1 & \text{homogeneous HDE} \\ 1 + \frac{\Omega_{\rm d}(a)}{\Omega_{\rm m}(a)}\Delta_{\rm d}(a)(1 + 3c^2_{\rm eff}) & \text{clustered HDE} \end{cases}, \tag{20}$$

where $c^2_{\rm eff}$ is the effective sound speed of the dark energy and $\Delta_d = \frac{1+w(a)}{1-3w(a)}$ [19,63]. For the homogeneous HDE model (hereafter HHDE), we have (see also Ref. [19])

$$\{M_0, M_1, H_1, X_1\} = \left\{1, 0, \frac{3w_\infty}{2}, -3w_\infty\right\},$$

where $w_\infty \simeq -1/3$, while the asymptotic value of the growth index becomes $\gamma_\infty = \frac{4}{7}$. The likelihood

analysis of Ref. [32] provides $\Omega_{m0} = 0.311 \pm 0.003$ and $s = 0.654 \pm 0.006$, from which we get $(\gamma_0, \gamma_1) \simeq (0.558, 0.013)$.

Moreover, for clustered HDE (hereafter CHDE) we find

$$\{M_0, M_1, H_1, X_1\} = \left\{1, -\frac{(1+3c_{\rm eff}^2)}{3}, \frac{3{\rm w}_\infty}{2}, -3{\rm w}_\infty\right\},$$

and hence

$$\gamma_\infty = \frac{3(1-c_{\rm eff}^2)}{7}.$$

Notice that we impose $c_{\rm eff}^2 = 0$, which means that the sound horizon is small with respect to the Hubble radius, and thus DE perturbations grow in a similar fashion to matter perturbations [64,65].

(5) **$f(T)$ gravity model (f_TCDM model):** Among the large body of $f(T)$ gravity models here, we focus on the power-law scenario first introduced by Bengochea and Ferraro [66], with $f(T) = \alpha(-T)^b$, where $\alpha = (6H_0^2)^{1-b}\frac{\Omega_{F0}}{2b-1}$. In this case, the dimensionless Hubble parameter is

$$E^2(a,b) = \Omega_{m0}a^{-3} + \Omega_{d0}E^{2b}(a,b), \quad (21)$$

and

$$\frac{d\ln E}{d\ln a} = -\frac{3}{2}\frac{\Omega_m(a)}{[1-bE^{2(b-1)}\Omega_{d0}]}, \quad (22)$$

where $\Omega_{d0} = 1 - \Omega_{m0}$. Since $b \ll 1$ [67], we use the approximation of Nesseris *et al.* [68] in order to simplify Eqs. (21) and (22), namely

$$E^2(a,b) \simeq E_\Lambda^2(a) + \Omega_{d0}\ln[E_\Lambda^2(a)]b + \cdots, \quad (23)$$

$$\frac{d\ln E}{d\ln a} \simeq -\frac{3}{2}\Omega_m(a)\left[1 + \frac{\Omega_{d0}b}{E_\Lambda^2(a)} + \cdots\right]. \quad (24)$$

For this geometrical model we have $\tilde{\nu} = 1$, while the quantity μ is given by (see Ref. [20] and references therein)

$$\mu(a) = \frac{1}{1 + \frac{b\Omega_{d0}}{(1-2b)E^{2(1-b)}}} \quad (25)$$

or

$$\mu(a) \simeq 1 - \frac{\Omega_{d0}}{E_\Lambda^2(a)}b + \cdots. \quad (26)$$

Using the above expressions, we are ready to compute the growth index coefficients of Eqs. (9) and (10) (see also Ref. [20]):

$$\{M_0, M_1, H_1, X_1\} = \left\{1, b, -\frac{3(1-b)}{2}, 3(1-b)\right\},$$

from which we derive

$$\gamma_\infty = \frac{6}{11-6b}.$$

Obviously, for $b = 0$ we recover the ΛCDM value $6/11$.

(6) **$f(R)$ gravity (f_RCDM model):** We would like to finish the presentation of the cosmological models with the $f(R)$ model introduced by Hu and Sawicki. As proposed by Basilakos *et al.* [69], the Lagrangian of the current $f(R)$ model can be equivalently written as

$$f(R) = R - \frac{2\Lambda}{1 + (\frac{b\Lambda}{R})^n}, \quad (27)$$

where n is a parameter of the model (we set it to unity without loss of generality). Following the methodology of Ref. [69], the Hubble parameter is given in terms of a series expansion of the solution of the equations of motion around $b = 0$; i.e. ΛCDM, as

$$H^2(a) = H_\Lambda^2(a) + \sum_{i=1}^{M} b^i \delta H_i^2(a), \quad (28)$$

where H_Λ is the Hubble parameter of the concordance ΛCDM model. Notice that $\delta H_i^2(a)$ is a set of algebraic quantities that can be determined from the equations of motion; see Ref. [69]. Moreover, the latter authors found that if we keep the two first nonzero terms ($M = 2$) of the series, then the approximated Hubble parameter is in excellent agreement with that provided by the numerical solution. Investigating the growth index in this model is not an easy task, since the modified Newton's constant is a function of both the scale factor a and the scale k; i.e. $G_{\rm eff} = G_{\rm eff}(a,k)$ [70]. In particular, we have

$$\mu(a,k) = \frac{G_{\rm eff}(a,k)}{G_N} = \frac{1}{F}\frac{1 + 4\frac{k^2}{a^2}F_{,R}/F}{1 + 3\frac{k^2}{a^2}F_{,R}/F}, \quad (29)$$

where $F = f'(R)$, $F_{,R} = f''(R)$, and we have scaled Eq. (29) so that in the case of $b = 0$ (ΛCDM) we recover $\frac{G_{\rm eff}(a,k)}{G_N} = 1$ as we should. Here we follow Ref. [69] and set $k = 0.1h\,{\rm Mpc}^{-1} \simeq 300H_0$, while $\tilde{\nu}(a) = 1$.

Finally, in Ref. [13], one can see that the current $f(R)$ model predicts rather low and rather high values for the growth index parameters, $(\gamma_0, \gamma_1) \simeq (0.4, -0.2)$. Due to the k-dependence of the effective Newton's constant, in order to obtain the exact values of (γ_0, γ_1), we first need to solve Eq. (5) numerically in order to compute $\gamma_0 \simeq \frac{\ln(f(1))}{\ln(\Omega_{m0})}$, where $f(1)$ is the growth rate at $a = 1$, and then one can utilize Eq. (13) to estimate γ_1.

(7) **Dvali, Gabadadze and Porrati (DGP) gravity model:** In the framework of modified gravity models, we first introduce that of Dvali, Gabadadze and Porrati [71]. It is well known that the normalized Hubble parameter takes the form

$$E(a) = \sqrt{\Omega_{m0} a^{-3} + \Omega_{rc}} + \sqrt{\Omega_{rc}}, \qquad (30)$$

and thus $\Omega_{rc} = (1 - \Omega_{m0})^2/4$:

$$\frac{d \ln E}{d \ln a} = -\frac{3\Omega_m(a)}{1 + \Omega_m(a)}. \qquad (31)$$

Here the quantity $\mu(a) = G_{\rm eff}/G_N$ takes the form

$$\mu(a) = \frac{2 + 4\Omega_m^2(a)}{3 + 3\Omega_m^2(a)}$$

and $\tilde{\nu}(a) = 1$. Combining the above equations with Eqs. (9), (10), and (8), we obtain

$$\{M_0, M_1, H_1, X_1\} = \left\{1, \frac{1}{3}, -\frac{3}{4}, \frac{3}{2}\right\}$$

and $\gamma_\infty = \frac{11}{16}$ (see also Refs. [9,12]). Similar to the ΛCDM model, the DGP gravity model contains one free parameter, namely Ω.

(8) **Finsler-Randers dark energy model (FRDE):** The Finsler-Randers version of Finsler geometry has been used in order to build the FRDE model (see Ref. [72] and references therein). Interestingly, it has been shown that the cosmic expansion of this model coincides with that of DGP gravity [16]. Therefore, Eqs. (30) and (31) are also valid here, and thus we use $\Omega_m = 0.392 \pm 0.008$. Although the two dark energy models (FRDE and DGP) are identical at the background level, they deviate at the perturbation level, because for the FRDE model we are dealing with $\mu(a) = \tilde{\nu}(a) = 1$ [72]. In this case it has been found that [32]

$$\{M_0, M_1, H_1, X_1\} = \{1, 0, -\frac{3}{4}, \frac{3}{2}\},$$

which implies $\gamma_\infty = \frac{9}{16}$.

IV. TENSION WITH PLANCK AND PREVIOUS ANALYSES

At this point, we should stress that by performing the joint analysis of all the data, including the updated growth compilation "Gold-2017" of Ref. [33], we confirm the existence of a tension between the growth-rate and the Planck15 data which have been already observed, and also for other low-redshift probes, and those discussed in the literature (see Refs. [33,73,74]).

This tension was not so obvious in the previous analysis of Basilakos and Nesseris [32] for two reasons: First, the analysis was done in two steps by initially fitting the background to the SnIa, CMB, BAO and $H(z)$ data and then fixing these best-fit parameters $(\Omega_m, \Omega_b h^2, \ldots)$ before fitting the growth-rate data. Second, not only were the growth-rate data used an older compilation with much bigger errors, but the corrections required due to the Alcock-Paczynski effect, due to the different fiducial cosmologies assumed in the derivations of the data, were not implemented at the time, unlike in the current analysis or that of Ref. [33]. These corrections contribute only up to a few percent, but could in principle bias the results and are thus necessary.

In order to understand why this tension, but also the difference in the best-fit values of (γ_0, γ_1) from Ref. [32], occurs, we show in Fig. 1 the best-fit γ_0 for the ΛCDM model as a function of Ω_m for various values of the σ_8 parameter. As can be seen, for higher values of Ω_m the new $f\sigma_8$ data push the best-fit γ_0 to higher values as well—or in other words, they are positively correlated. This means that

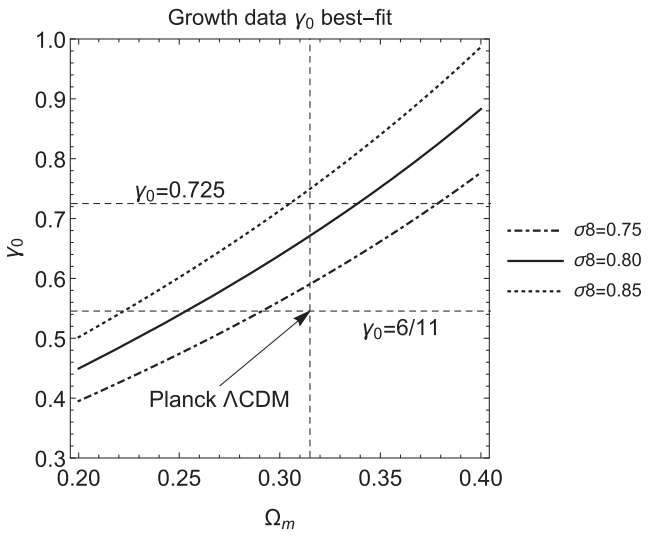

FIG. 1. The best-fit γ_0 for the ΛCDM model as a function of Ω_m for various values of the σ_8 parameter. As can be seen, the $f\sigma_8$ data push the best-fit γ_0 to higher values for higher Ω_m. This means that when a Planck cosmology of $\Omega_m = 0.315$ is used (shown with a vertical dashed line), then the best fit is in the region of $\gamma_0 \sim 0.73$, in contrast to lower values of Ω_m that prefer a value for the γ_0 parameter closer to $6/11$.

when the Planck cosmology of $\Omega_m = 0.315$ is used (shown in Fig. 1 with a vertical dashed line), then the best-fit growth index is in the range of $\gamma_0 \sim 0.73$, in contrast to lower values of Ω_m that prefer a value for the γ_0 parameter closer to $6/11 \simeq 0.545$.

Furthermore, with the small arrow we show the Planck ΛCDM values of $(\gamma_0, \Omega_m) = (6/11, 0.315)$, which is quite far from our best fit of $\gamma_0 = 0.725$. Also, it is important to note that the effect of the parameter σ_8 is quite strong, as it can strongly affect the value of the growth index. For example, as shown in Fig. 1, by changing σ between $\sigma_8 \in [0.75, 0.85]$, the growth index changes by roughly 30%. This is also part of the reason for the disagreement with Ref. [32], as the best-fit values of σ_8 in that case were quite lower than in this analysis.

Finally, this tension could be attributed to systematics in the low-redshift probes [73], new physics in the form of modifications of gravity and $G_{\rm eff}$ in particular [33], or even in the form of a suppression of power at small scales [75].

V. CONJOINED ANALYSIS WITH REAL AND MOCK DATA

In this section we implement the *conjoined method* of Ref. [21] in order to distinguish the dark energy models, by

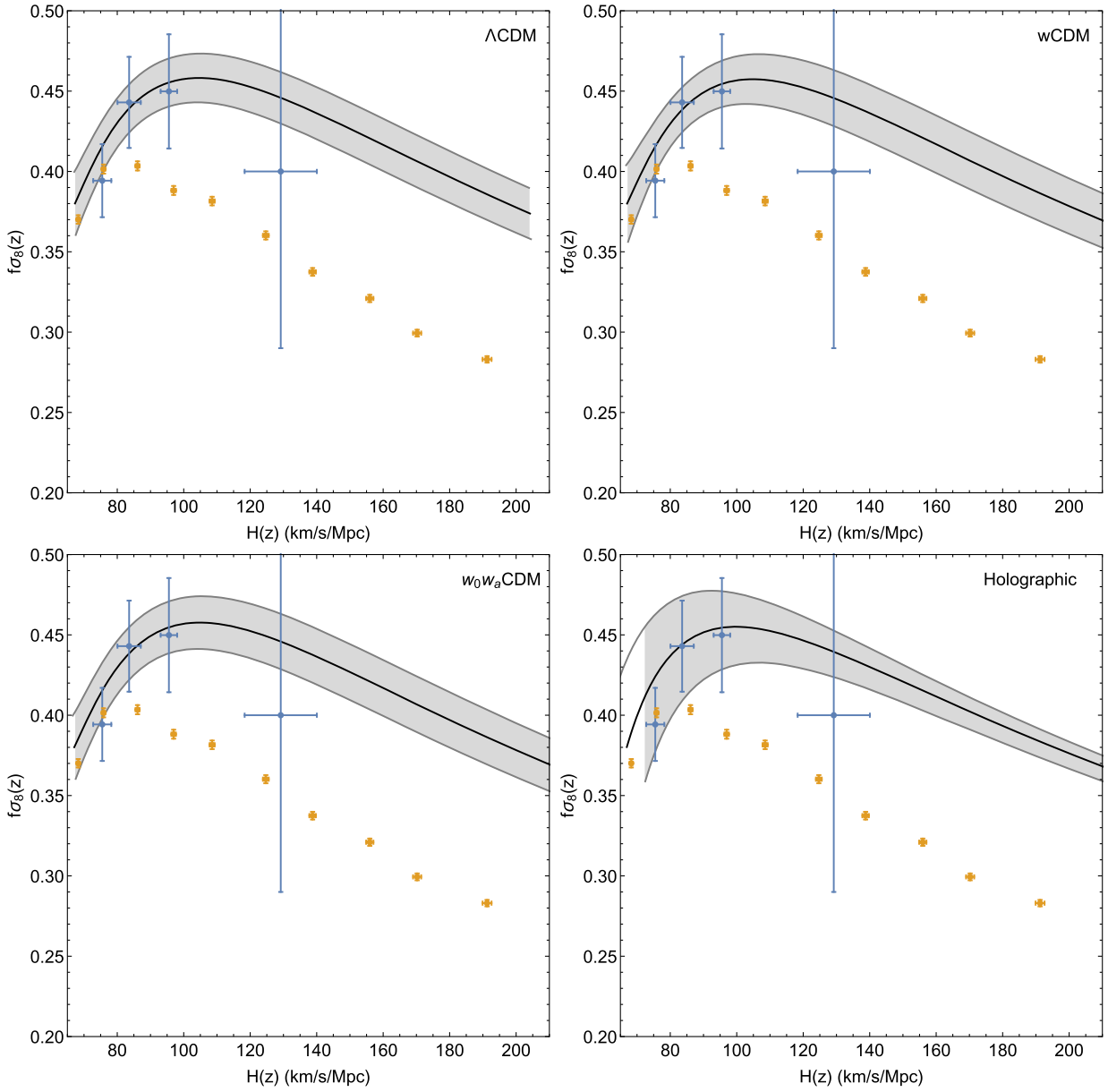

FIG. 2. The conjoined plots of the cosmic growth $f\sigma_8$ vs the cosmic expansion history $H(z)$ based on the real data (blue points) and mock data (yellow points), as described in the text, for the ΛCDM, wCDM, w_0w_aCDM and holographic models. We also show the 1σ error regions in grey.

placing constraints simultaneously on both the expansion history $H(z)$ and the growth of structure $f\sigma_8(z)$. Specifically, Ref. [21] proposed to utilize the expansion history together with the cosmic growth history, namely the joined analysis of H-$f\sigma_8$, as a tool for testing the performance of the dark energy models. Obviously, in order to obtain the conjoined histories diagram, it is essential to provide a proper collection of the H-$f\sigma_8$ data. Concerning the cosmic history, we use the latest cosmic chronometer $H(z)$ data (see Table I and references therein), while for the growth data we refer the reader to our Table II.

Therefore, assuming that the Universe is isotropic, our aim is to correlate the growth as measured in the form of $f\sigma_8(z)$ with that of the cosmic expansion via the Hubble measurements $H(z_h)$ from the cosmic chronometer data, which are measured in the range $0.07 \leq z_h \leq 2.34$ (see Table I). More specifically, we implement the following steps:

(1) We note that the maximum redshift for the $f\sigma_8$ data is $z_{max} = 1.4$; hence, we only keep the $H(z)$ data up to that redshift, so that we have a common sample in the same redshift range.

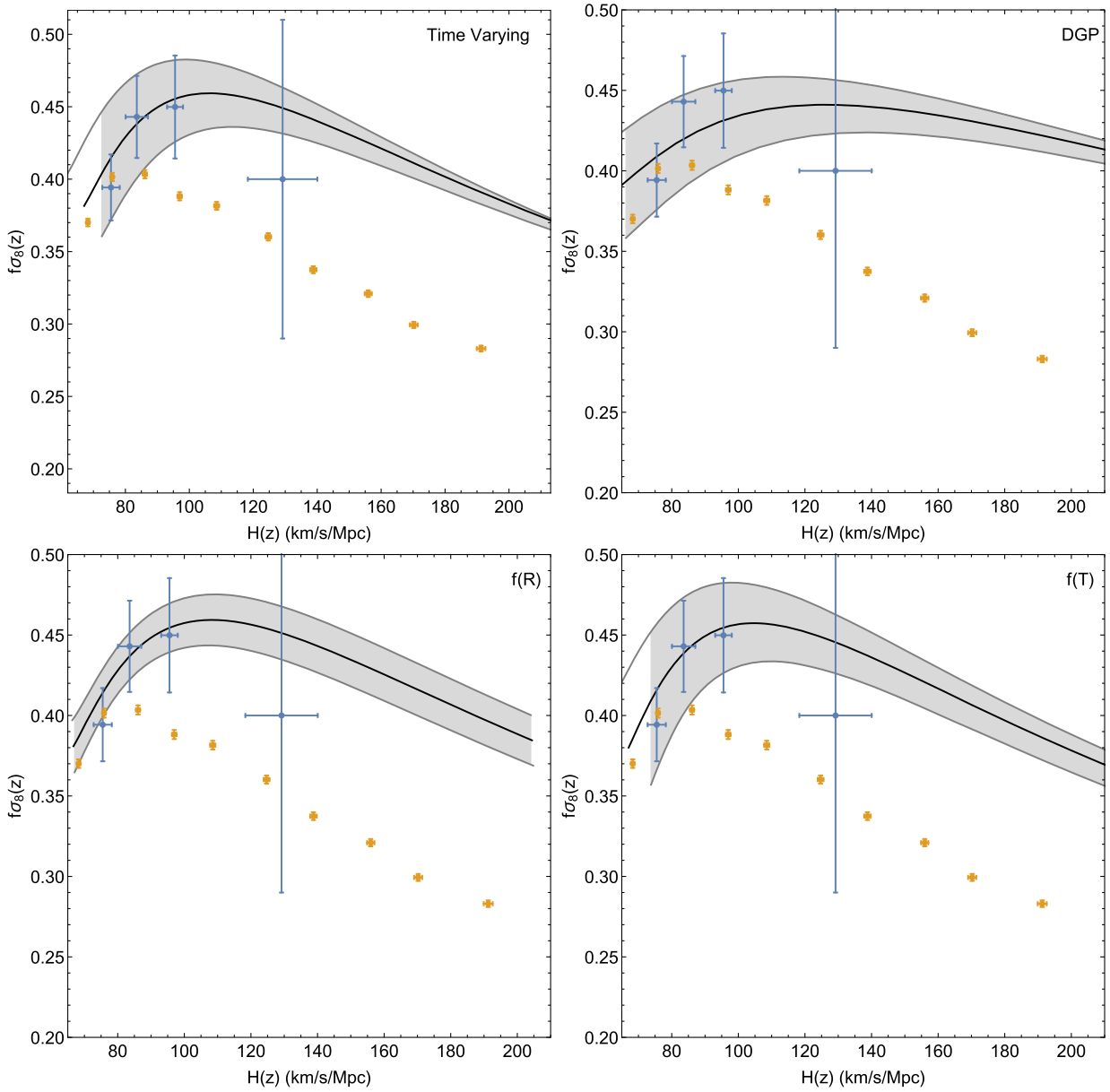

FIG. 3. The conjoined plots of the cosmic growth $f\sigma_8$ vs the cosmic expansion history $H(z)$ based on the real data (blue points) and mock data (yellow points), as described in the text, for the time-varying vacuum, DGP, $f(R)$ and $f(T)$ models. We also show the 1σ error regions in grey.

TABLE IV. The binned $H(z)$-$f\sigma_8(z)$ growth data based on the original data of Tables I and II.

Bins	$H(z)$	$f\sigma_8(z)$
$0 \leq z < 0.28$	75.489 ± 2.718	0.394 ± 0.023
$0.28 \leq z < 0.56$	83.572 ± 3.501	0.443 ± 0.028
$0.56 \leq z < 0.84$	95.540 ± 2.482	0.449 ± 0.036
$0.84 \leq z < 1.12$	129.189 ± 10.862	0.400 ± 0.110

(2) We then split both the $f\sigma_8$ and the remaining $H(z)$ data into four equal bins[3] and weight the data according to their errors; see Ref. [76].
(3) For the combined sample we perform a statistical analysis, and by using the models and best-fit parameters as mentioned in the previous section, we make the conjoined H-$f\sigma_8$ curves as seen in Figs. 2 and 3, along with real and mock data.
(4) For the region defined by the 1σ errors of the best-fit theoretical models in the $H(z)$-$f\sigma_8(z)$ space, we also calculate the figure of merit (FoM), which is equal to the inverse of the enclosed area up to the maximum redshift range covered by both models. Then we rank the models according to their constraining power (see Table V). Note that the higher the FoM, the more constraining the model becomes.

Following the previous steps, we now show in Figs. 2 and 3 the conjoined plots of the cosmic growth $f\sigma_8(z)$ vs the cosmic expansion history $H(z)$ based on the real data (blue points) and mock data (yellow points), for the ΛCDM, wCDM, w_0w_aCDM, holographic, time-varying vacuum, DGP, $f(R)$ and $f(T)$ models. We also show the 1σ error regions in grey, and we use them later on to calculate the $H(z)$-$f\sigma_8(z)$ FoM. In these plots, the real data of Table II were split into four equally spaced bins, given in Table IV, while the mock data (yellow points) were based on an LSST-like survey with data in the range $z \in [0, 2]$ and a Planck15 best-fit cosmology with $\Omega_m = 0.317$, $H_0 = 67.2$ km/s/Mpc, $w = -1$ and $\sigma_8 = 0.687$. Finally, the mock data were slit into ten equally spaced redshift bins.

As can be seen, there is little difference between the theoretical curves of the various models, which is in agreement with our results in Ref. [32]. One exception however, is the DGP model, which seems to be in strong tension with the data, having a $\delta\chi^2 \sim 100$ with the rest of the models, again confirming our earlier analysis. However, an LSST-like survey, as seen by the mock data (yellow points in Figs. 2 and 3), will be able to discriminate the models and provide stringent constraints on the cosmic growth and expansion history. Furthermore, a survey like this will be able to shed light on the existing tension with Planck by providing data points with very small errors and by minimizing the systematics that occur by combining data from many surveys.

[3]We found by trial and error that this is the optimal number of bins given the number of data in both sets.

TABLE V. The FoM in the $H(z)$-$f\sigma_8(z)$ parameter space in descending order, from higher FoM (more constraining) to lower FoM (less constraining).

Model	FoM
ΛCDM	0.3767
f_RCDM	0.3733
wCDM	0.3589
CPL	0.3488
HDE	0.2509
Λ_tCDM	0.2416
DGP	0.2288
FRDE	0.2288
f_TCDM	0.2223

We also calculate the FoM in the $H(z)$-$f\sigma_8(z)$ parameter space in order to assess how constraining the joined analysis of these data can be. We have defined the FoM as the inverse of the enclosed area of the 1σ error regions in Figs. 2 and 3 up to the common maximum redshift $z_{\max} = 1.4$. We then rank all the models according to their constraining power, noting that the higher the FoM, the more constraining the model becomes.

The result of this comparison is shown in Table V, where we notice that the ΛCDM model seems to be much more constraining, followed up closely by the f_RCDM and wCDM models. As mentioned before, the DGP/Finsler models are at the bottom of the ranking, with less than half the constraining power of the rest of the models. Finally, we note that the $f(T)$ model is also at the bottom of the list, something which allows us to discriminate it from the rest of the models even though the model itself is just a perturbation around ΛCDM. Therefore, the technique of the conjoined analysis of both the $H(z)$ and $f\sigma_8(z)$ can in principle discriminate some modifications of gravity from ΛCDM.

VI. CONCLUSIONS

In our present study we implemented the H-$f\sigma_8$ conjoined method of Ref. [21] in order to test the viability of a large family of DE models, including the ΛCDM, wCDM, w_0w_aCDM, holographic, time-varying vacuum, DGP, $f(R)$ and $f(T)$ models. First, we combined the available cosmic chronometer and growth data, given in Tables I and II, respectively, and then we identified a common subsample which extends up to redshift $z_{\max} = 1.4$, and we binned the corresponding data. With this subsample and using the best-fit parameters of the models, as described in Table III, we then performed the conjoined analysis of the H-$f\sigma_8$ parameters, the results of which can be seen in Figs. 2 and 3.

We found that even though there is little difference between the theoretical curves of most of the models,

something which is in agreement with our previous results in Ref. [32], we note that the DGP/Finsler class of models seems to be in somewhat strong tension with the data. Also, by analyzing all the data [CMB, SnIa, BAO, growth and $H(z)$], we also observed a strong tension between the growth data and Planck. As mentioned, this tension pushes the values of the growth index γ_0 and σ_8 to be higher than our previous separate analysis.

Furthermore, using a set of mock data, based on an LSST-like survey with Planck15 cosmological parameters, i.e. the yellow points in Figs. 2 and 3, we determined that in the near future we will be able to discriminate the models and provide even more stringent simultaneous constraints on the cosmic growth and expansion history.

Using our analysis, we could also quantify the level of the constraining power of these models by using the FoM on the conjoined parameter space of H-$f\sigma_8$. The results of this analysis were shown in Table V. By ranking the models according to their performance, noting that the higher the FoM, the more constraining the model becomes, we found that the ΛCDM model seems to be the most constraining, followed up closely by the f_RCDM and wCDM models. Again, in agreement with our previous results, we also found that the DGP/Finsler models are at the bottom of the ranking, with almost half the constraining power of the rest of the models.

Finally, we observed that the $f(T)$ model is also at the bottom of the list, something which hints that the conjoined analysis is capable of discriminating such modified gravity models from ΛCDM, thus proving to be a useful tool given the plethora of dark energy or modified gravity models that are currently available, but also the wealth of data expected from the upcoming surveys in the next decade or so.

ACKNOWLEDGMENTS

The authors would like to thank E. V. Linder for fruitful discussions. S. B. acknowledges support by the Research Center for Astronomy of the Academy of Athens in the context of the program "*Testing general relativity on cosmological scales*" (Ref. No. 200/872). S. N. acknowledges support by the Research Project of the Spanish MINECO under Grant No. FPA2013-47986-03-3P, the Centro de Excelencia Severo Ochoa Program through Grant No. SEV-2012-0249, and the Ramón y Cajal program through Grant No. RYC-2014-15843.

[1] P. A. R. Ade *et al.* (Planck Collaboration), Astron. Astrophys. **594**, A13 (2016).
[2] E. J. Copeland, M. Sami, and S. Tsujikawa, Int. J. Mod. Phys. D **15**, 1753 (2006).
[3] R. R. Caldwell and M. Kamionkowski, Annu. Rev. Nucl. Part. Sci. **59**, 397 (2009).
[4] T. Clifton, P. G. Ferreira, A. Padilla, and C. Skordis, Phys. Rep. **513**, 1 (2012).
[5] T. Okumura *et al.*, Publ. Astron. Soc. Jpn. **68**, 38 (2016).
[6] V. Silveira and I. Waga, Phys. Rev. D **50**, 4890 (1994).
[7] L.-M. Wang and P. J. Steinhardt, Astrophys. J. **508**, 483 (1998).
[8] E. V. Linder and A. Jenkins, Mon. Not. R. Astron. Soc. **346**, 573 (2003).
[9] E. V. Linder, Phys. Rev. D **70**, 023511 (2004).
[10] S. Nesseris and L. Perivolaropoulos, Phys. Rev. D **77**, 023504 (2008).
[11] A. Lue, R. Scoccimarro, and G. D. Starkman, Phys. Rev. D **69**, 124015 (2004).
[12] Y. Gong, Phys. Rev. D **78**, 123010 (2008).
[13] R. Gannouji, B. Moraes, and D. Polarski, J. Cosmol. Astropart. Phys. 02 (2009) 034.
[14] S. Tsujikawa, R. Gannouji, B. Moraes, and D. Polarski, Phys. Rev. D **80**, 084044 (2009).
[15] L. Boubekeur, E. Giusarma, O. Mena, and H. Ramrez, Phys. Rev. D **90**, 103512 (2014).
[16] S. Basilakos and P. Stavrinos, Phys. Rev. D **87**, 043506 (2013).
[17] S. Basilakos and J. Sol, Phys. Rev. D **92**, 123501 (2015).
[18] A. Mehrabi, S. Basilakos, and F. Pace, Mon. Not. R. Astron. Soc. **452**, 2930 (2015).
[19] A. Mehrabi, S. Basilakos, M. Malekjani, and Z. Davari, Phys. Rev. D **92**, 123513 (2015).
[20] S. Basilakos, Phys. Rev. D **93**, 083007 (2016).
[21] E. V. Linder, Astropart. Phys. **86**, 41 (2017).
[22] M. Moresco and F. Marulli, arXiv:1705.07903.
[23] H. F. Stabenau and B. Jain, Phys. Rev. D **74**, 084007 (2006).
[24] J.-P. Uzan, Gen. Relativ. Gravit. **39**, 307 (2007).
[25] S. Tsujikawa, K. Uddin, and R. Tavakol, Phys. Rev. D **77**, 043007 (2008).
[26] S. Nesseris, Phys. Rev. D **79**, 044015 (2009).
[27] P. J. E. Peebles, *Principles of Physical Cosmology* (Princeton University Press, Princeton, NJ, 1993).
[28] H. Steigerwald, J. Bel, and C. Marinoni, J. Cosmol. Astropart. Phys. 05 (2014) 042.
[29] D. Polarski and R. Gannouji, Phys. Lett. B **660**, 439 (2008).
[30] A. Bueno belloso, J. Garcia-Bellido, and D. Sapone, J. Cosmol. Astropart. Phys. 10 (2011) 010.
[31] C. Di Porto, L. Amendola, and E. Branchini, Mon. Not. R. Astron. Soc. **419**, 985 (2012).
[32] S. Basilakos and S. Nesseris, Phys. Rev. D **94**, 123525 (2016).
[33] S. Nesseris, G. Pantazis, and L. Perivolaropoulos, Phys. Rev. D **96**, 023542 (2017).
[34] M. Moresco, L. Pozzetti, A. Cimatti, R. Jimenez, C. Maraston, L. Verde, D. Thomas, A. Citro, R. Tojeiro, and D. Wilkinson, J. Cosmol. Astropart. Phys. 05 (2016) 014.
[35] R.-Y. Guo and X. Zhang, Eur. Phys. J. C **76**, 163 (2016).

[36] C. Zhang, H. Zhang, S. Yuan, T.-J. Zhang, and Y.-C. Sun, Res. Astron. Astrophys. **14**, 1221 (2014).
[37] D. Stern, R. Jimenez, L. Verde, M. Kamionkowski, and S. A. Stanford, J. Cosmol. Astropart. Phys. 02 (2010) 008.
[38] M. Moresco *et al.*, J. Cosmol. Astropart. Phys. 08 (2012) 006.
[39] C.-H. Chuang and Y. Wang, Mon. Not. R. Astron. Soc. **435**, 255 (2013).
[40] C. Blake *et al.*, Mon. Not. R. Astron. Soc. **425**, 405 (2012).
[41] L. Anderson *et al.* (BOSS Collaboration), Mon. Not. R. Astron. Soc. **441**, 24 (2014).
[42] M. Moresco, Mon. Not. R. Astron. Soc. **450**, L16 (2015).
[43] T. Delubac *et al.* (BOSS Collaboration), Astron. Astrophys. **574**, A59 (2015).
[44] D. Huterer, D. Shafer, D. Scolnic, and F. Schmidt, J. Cosmol. Astropart. Phys. 05 (2017) 015.
[45] S. J. Turnbull, M. J. Hudson, H. A. Feldman, M. Hicken, R. P. Kirshner, and R. Watkins, Mon. Not. R. Astron. Soc. **420**, 447 (2012).
[46] M. J. Hudson and S. J. Turnbull, Astrophys. J. **751**, L30 (2012).
[47] M. Davis, A. Nusser, K. Masters, C. Springob, J. P. Huchra, and G. Lemson, Mon. Not. R. Astron. Soc. **413**, 2906 (2011).
[48] M. Feix, A. Nusser, and E. Branchini, Phys. Rev. Lett. **115**, 011301 (2015).
[49] C. Howlett, A. Ross, L. Samushia, W. Percival, and M. Manera, Mon. Not. R. Astron. Soc. **449**, 848 (2015).
[50] Y.-S. Song and W. J. Percival, J. Cosmol. Astropart. Phys. 10 (2009) 004.
[51] C. Blake *et al.*, Mon. Not. R. Astron. Soc. **436**, 3089 (2013).
[52] L. Samushia, W. J. Percival, and A. Raccanelli, Mon. Not. R. Astron. Soc. **420**, 2102 (2012).
[53] A. G. Sanchez *et al.*, Mon. Not. R. Astron. Soc. **440**, 2692 (2014).
[54] C.-H. Chuang *et al.*, Mon. Not. R. Astron. Soc. **461**, 3781 (2016).
[55] A. Pezzotta *et al.*, Astron. Astrophys. **604**, A33 (2017).
[56] S. Basilakos and A. Pouri, Mon. Not. R. Astron. Soc. **423**, 3761 (2012).
[57] M. Chevallier and D. Polarski, Int. J. Mod. Phys. D **10**, 213 (2001).
[58] E. V. Linder, Phys. Rev. Lett. **90**, 091301 (2003).
[59] I. L. Shapiro and J. Sola, J. High Energy Phys. 02 (2002) 006.
[60] C. Espana-Bonet, P. Ruiz-Lapuente, I. L. Shapiro, and J. Sola, J. Cosmol. Astropart. Phys. 02 (2004) 006.
[61] Y. J. Ng, Phys. Rev. Lett. **86**, 2946 (2001); **88**, 139902(E) (2002).
[62] P. Horava and D. Minic, Phys. Rev. Lett. **85**, 1610 (2000).
[63] R. C. Batista and F. Pace, J. Cosmol. Astropart. Phys. 06 (2013) 044.
[64] J. Garriga and V. F. Mukhanov, Phys. Lett. B **458**, 219 (1999).
[65] C. Armendariz-Picon, T. Damour, and V. F. Mukhanov, Phys. Lett. B **458**, 209 (1999).
[66] G. R. Bengochea and R. Ferraro, Phys. Rev. D **79**, 124019 (2009).
[67] E. V. Linder, Phys. Rev. D **81**, 127301 (2010); **82**, 109902(E) (2010).
[68] S. Nesseris, S. Basilakos, E. N. Saridakis, and L. Perivolaropoulos, Phys. Rev. D **88**, 103010 (2013).
[69] S. Basilakos, S. Nesseris, and L. Perivolaropoulos, Phys. Rev. D **87**, 123529 (2013).
[70] S. Tsujikawa, Phys. Rev. D **76**, 023514 (2007).
[71] G. R. Dvali, G. Gabadadze, and M. Porrati, Phys. Lett. B **485**, 208 (2000).
[72] P. C. Stavrinos, A. P. Kouretsis, and M. Stathakopoulos, Gen. Relativ. Gravit. **40**, 1403 (2008).
[73] S. Joudaki *et al.*, Mon. Not. R. Astron. Soc. **465**, 2033 (2017).
[74] S. Basilakos, Mon. Not. R. Astron. Soc. **449**, 2151 (2015).
[75] M. Kunz, S. Nesseris, and I. Sawicki, Phys. Rev. D **92**, 063006 (2015).
[76] S. Nesseris and D. Sapone, Phys. Rev. D **90**, 063006 (2014).